AN APPROACH TO AUTOMATIC CLASSIFICATION OF AURORAS BASED ON ALL-SKY CAMERAS OBSERVATION DATA

© 2025 A.V. Vorobev[a], *, A.N. Lapin[b], **, G.R. Vorobeva[b], ***

[a]*Geophysical Center of the RAS, Moscow, Russia*

[b]*Ufa University of Science and Technology, Ufa, Russia*

**e-mail:geomagnet@list.ru*

***e-mail: meccos160@yandex.ru*

****e-mail: gulnara.vorobeva@gmail.com*

Received April 21, 2025

Revised May 19, 2025

Accepted May 22, 2025

Abstract. An original approach to automatic classification of auroras by machine identification of images received from sky photo recorders, also called all-sky imagers, is proposed. A total of 163899 sky images within the auroral oval (Kola Peninsula, Russia) were selected at 10-minute intervals over a 10-year period. We propose an intelligent information system designed to classify each acquired image into one of seven predefined categories. Analysis of the quality metrics of the system built on the basis of the ResNet50 neural network architecture showed the accuracy of the classification at the level of 96 %, which is practically unattainable in the conditions of manual data processing on samples of such a volume. The result of automatic classification of sky images based on the proposed system is available at the link: (https://disk.yandex.ru/i/76OMyWR4YyVYuw).

Keywords: *auroras, automatic classification, computer vision*

DOI: 10.31857/S00167940250515e6

1. INTRODUCTION

It is known that the highest risks of technosphere safety reduction associated with the effects of space weather on technical systems and networks are determined within the boundaries of the auroral oval - a belt of intense luminosity created by the intrusion of electrons from near-Earth space into the atmosphere [Vorobev et al., 2022; Pilipenko et al., 2023]. At the same time, for the majority of high-latitude regions of Russia (due to the lack of reliable sources of operational information on the local geomagnetic situation), auroras remain practically the only publicly available indicator of space weather conditions.

There are studies indicating that the area of polar lights observation, their luminescence intensity and morphology are closely related to the power of manifestation of space weather effects

on high-latitude technological systems [Vorobev et al., 2024]. It was shown that the most probable level of geoinduced currents (GIT) J_{VKH} registered at Vykhodnoy station (68.83° N, 33.08° E) at simultaneous observation of auroras in the north, in the zenith and in the south of the sky relative to Lovozero station (67.97° N, 35.02° E) is 0.08, 0.23 and 0.68 A, respectively. The posterior probability of the event $J_{VKH} > 2$ A at observation of auroras in the north of the sky is 5.78%, while the probability of exceeding this level at auroras in the zenith and in the south is 10.04% and 14.93%, respectively. In the absence of auroras, the probability of J_{VKH} reaching the level of 2 A does not exceed 0.26%, and the probability of exceeding 3 A is practically equal to zero.

Fig. 1.

We present data that during December 21, 2016 (Fig. 1), the minute-average GIT level was up to 0.1 A for periods of no auroras (12:48 UT), 0.7 A for diffuse auroras (17:07 UT), and 1.34 and 13.06 A for intense auroras of the "arc" (15:35 UT) and "vortex" (15:43 UT) types, respectively [Vorobev et al., 2024].

The declared results were obtained through manual processing and classification of 1921 ascaplots [Vorobev et al., 2023], which corresponds to 92208 episodes of 30-min skywave observations for 2011-2021. However, as practice has shown, this approach to data representation has practically lost its relevance and is of little use in the tasks of analyzing poorly structured information collected over half a century. In turn, constantly developing computer vision technologies demonstrate the potential for detecting hidden trends and regularities within the observed system over large time intervals. Thus, for example, in a conceptually similar way (meaning the concept of "Citizen science"), it is possible to detect hidden trends and patterns within the observed system over large time intervals. [Steven et al., 2019], which eliminates the need for a deep dive into the subject area), in 2018, a previously unknown type of atmospheric phenomena STEVE (from STEVE - Strong Thermal Emission Velocity Enhancement) was discovered, which has the appearance of a long light streak in the sky [MacDonald et al., 2018; Gallardo-Lacourt et al., 2018].

In a broader sense, the development of these technologies in the subject area, in addition to clarifying the conditions of occurrence and evolution of extreme geophysical events in the upper ionosphere, can contribute to improving the efficiency of management of complex technical systems deployed inside the Arctic Zone of the Russian Federation (AZRF).

Thus, the aim of this work is to develop an approach and an information system for automatic classification of auroras on the basis of domestic long-term sky observation data inside the auroral oval boundaries, as well as to analyze and assess the relevance of the results obtained.

It is expected that the results obtained here will open the possibility of conducting a series of additional more sophisticated studies consisting in comparing the morphology of polar lights with data from magnetometers, ionosondes, or GIT observations, in the corresponding subregion.

2. INITIAL DATA AND THEIR PRELIMINARY PROCESSING

The data for the 10-year period (2015-2024) of the highest-quality optical observations of the auroras by the cameras of Obs. Lovozero Observatory (LOZ). It should be noted that the Lovozero Obs. Lovozero Observatory (LOZ) is part of the Polar Geophysical Institute (PGI) and is practically the only station on the territory of the Russian Federation that has been continuously and for a long time conducting observations and recording of auroras, magnetic field variations and other geophysical effects of high latitudes caused by processes in the Earth's magnetosphere, ionosphere and atmosphere.

The observational data published in the public domain (http://aurora.pgia.ru:8071/?p=2) are RGB images with a resolution of 600×600 px and a sampling step of 10 c. Correlating the selected volume of graphic information with the computing power required for its processing and taking into account the dynamics of the observed events, it is proposed to consider images with a sampling step of 10 min. Also at the stage of preprocessing the images were scaled to the size of 224×224 px, which led to a reduction in their volume, and as a result - a significant increase in the training speed of the neural network model.

Thus, after preprocessing, we have skywave observation data from 04.12.2015 (19:00) to 27.04.2024 (23:10) UTC, representing 163899 consecutively registered non-repeating images with a total volume of ~8 GB.

3. DATA CLASSIFICATION METHODOLOGY OF OPTICAL OBSERVATIONS OF THE SKY IN THE AURORAL ZONE

To date, there is no standardized approach to classifying the structure and morphology of auroras. Specialists, as a rule, distinguish arcs, diffuse and discrete auroras (Table 1), while the terminology of one and the same type of auroras can differ significantly among different authors (e.g., [Nanjo et al., 2022] and [Sado et al., 2022]). In addition to belonging auroras to one of the deterministic types, images from photorecorders as such are often subjected to the classification procedure, resulting in additional classes that are not directly related to the auroras or the state of the ionosphere: full or partial cloudiness, lunar or solar illumination, clear sky, cloudiness, appearance of artifacts, etc.

Table 1.

As it follows from Table 1, the following set of sky states is most often proposed: arc, diffuse or discrete aurora, and no aurora or cloudiness. Less common is the "Moon" class, corresponding to lunar illumination of the image.

Pursuing the goal of classifying the auroras by means of all-sky camera data, the most significant are the classes that explicitly characterize the presence and morphology of the auroras in

the observation area. Acting in accordance with the logic of some previous studies, the available images are proposed to be categorized as follows**.**

1. Clear sky / no aurora (CNA from English Clear / No aurora) - images in which no auroras are unambiguously observed.

2. Discrete aurora (Discrete) - images with a pronounced and in some places discontinuous structure of the aurora resembling a spiral or vortex with brightness exceeding the brightness of background stars.

3. Arc radiance or arc (Arc) - images that have one or two pronounced horizontal arcs of radiance.

4. Diffuse radiance (Diffuse) - images that show large areas of radiance with blurred edges. The brightness of the auroras is comparable to or less than the brightness of the background stars.

5. Horizon auroras - images in which most of the aurora is located near or below the horizon, making it difficult to accurately identify the actual structure of the aurora.

6. Aurora but Cloudy (AC from Aurora but Cloudy) - images in which glow is observed in cloudy conditions, indicating the potential presence of aurora borealis, but, due to blurred geometry, it is not possible to unambiguously attribute it to one of the previously named classes.

7. Defective images (Broken) - images, which have strong noise and/or other artifacts due to hardware or software failures.

This classification is characterized by the presence of two new classes: "shines over the horizon" and "defective images". The first of these is designed to deal with the oversaturation of the "arc" class, visually similar to auroras near the horizon (Fig. *2d*), but strictly speaking, they are not. The second one - "defective images" is necessary for filtering artifacts that make up 4-5% of the total number of images (Fig. *2g*).

Further, the expert group processed and brought 92987 images - 57% of the total number of available photographs of the sky - into compliance with the proposed classification. The ratio between the images - representatives of each class is shown in Table 2.

Table 2.

Fig. 2.

Fig. 2 shows the characteristic representatives of the declared classes of images registered by obs. LOZ.

In cases of superposition of aurora types (Fig. 3) on one image, the class identification is proposed to be performed by the hierarchical method based on the average brightness value of images: Discrete => Arc => Diffuse => Horizon. An exception to this rule are images of auroras near the horizon whose geometry only resembles an arc, i.e., the conclusion about the real structure of the glow is ambiguous. In such cases, the event is classified as "auroras beyond the horizon". In case of

difficulty in identification by experts of a glow belonging to one of the presented classes, the image was ignored.

Fig. 3.

4. FORMATION OF TRAINING AND TEST SAMPLES

The manually partitioned 92987 images were divided into training and test samples in the ratio of 8:2, respectively. To increase the number of inputs, image mirroring with respect to the vertical (north– south) axis was used [Shorten et al., 2019]. Experience shows that the use of other data augmentation techniques can distort the information reflecting the morphological features of the polar lights evolution. Thus, for example, image mirroring relative to the horizontal (west– east) axis or image rotation by an arbitrary angle can provoke the loss of the trend of the appearance of more frequent and pronounced auroras in the northern region of the observed part of the sky. In turn, cropping or fragmentation of the image may cause loss of information about the relative position of the horizon line in the image and aggravate the problem of separating the classes of "arc" and "aurora borealis" types.

5. SYNTHESIS AND VALIDATION OF A NEURAL NETWORK MODEL FOR AUTOMATIC CLASSIFICATION OF SKYLINE PHOTOREGISTRATION RESULTS

The deep convolutional neural network architecture ResNet50 [He et al., 2016], pre-trained on the Imagenet dataset [Deng et al., 2009], consisting of 50 layers organized into 6 basic blocks, was used in this work (Fig. 4). The use of residual links in ResNet50 facilitates efficient training of the deep network to bypass the problem of fading gradients [Glorot and Bengio, 2010], which provides consistent best results relative to its counterparts: ResNet-18, AlexNet, VGG-19, etc. [Nanjo et al., 2022; Kvammen et al., 2020; Endo and Matsumoto, 2022, etc.].

Fig. 4.

According to this architecture, an image (224 px × 224 px × 3 channels) is received at the input of the network (224 px × 224 px × 3 channels), followed by a convolution block and three sequential operations: filtering the data through convolution, batch normalization, and applying nonlinear ReLU activation [Yarotsky, 2017], which allows iteratively finding important visual patterns (e.g., bright arc radiance boundaries). Next, a max-pooling layer is used, reducing spatial resolution, screening out less significant details, and focusing on dominant features. After passing the main block of residual layers in the Avg Pool block (Fig. 4), the data are averaged and fed to the final full-link layer responsible for classification. The result is processed by the softmax activation function converting the outputs into probability scores for each class. The class with the highest probability is identified as the final class.

Table 3.

Table 3 presents the mismatch matrix of the classification result obtained on a test sample of 18,557 images.

A more detailed analysis of the data (Table 3) indicates the following aspects.

- No radiance (CNA) and defective images (Broken) are identified with the highest accuracy: 99.4% and 99.8%, respectively. Although in classification tasks approaching 100% accuracy is usually unattainable, in this case such values are explained by the definition of the class itself. In the case of CNA, the situation is different. False identification of this class occurs in 7.5% of cases during diffuse brightening and in 6% of "brightening and cloudy" cases.

- The identification of arc, discrete auroras and auroras over the horizon has a rather high level of accuracy: 92.9, 89.7 and 92.2%, respectively. Here, false identification of the arc during the auroras over the horizon is observed in 2.6% of cases. In addition, 7.1% of discrete auroras overlap with arc auroras, caused by combined cases, which are processed according to the algorithm proposed above, or by the simultaneous presence of two or more arcs.

- Diffuse auroras are successfully identified only in 75.2% of cases, which is initially due to the fuzzy features of their determination at the data partitioning stage.

In multi-class image classification tasks, the weighted metrics Precision, Recall and F1 are key metrics to evaluate the quality of the resulting model. Compared to the simple use of Accuracy, they provide a more detailed picture of the imbalance of the radiance image classes.

$$Recall_w = \sum_{k=1}^{K} \frac{TP_k}{TP_k+FN_k} W_k; \quad (1)$$

$$Precision_w = \sum_{k=1}^{K} \frac{TP_k}{TP_k+FP_k} W_k; \quad (2)$$

$$F1_w = \sum_{k=1}^{K} \frac{2TP_k}{2TP_k+FN_k+FP_k} W_k, \quad (3)$$

where $Recall_w$, $Precision_w$ and $F1_w$ are the weighted metrics *Recall*, *Precision* and F1, respectively; TP_k, FP_k, FN_k, TN_k are the true-positive, false-positive, false-negative and true-negative, respectively, elements of the sample with respect to class k [De Diego et al., 2022].

The weight of the *k-th* class W_k was determined from the ratio of the number of labeled images:

$$W_k = \frac{O_k}{\sum_{l=1}^{K} O_k}, \quad (4)$$

where O_k is the number of labeled images.

Table 4 shows the weighted and macro-averaged quality metrics of the classification system obtained by equating the value of W_k to *1/K*.

The result of automatic image classification based on the proposed system is available at: (https://disk.yandex.ru/i/76OMyWR4YyVYuw).

Table 4.

6. STATISTICAL ANALYSIS OF CLASSIFICATION RESULTS

Fig. 5 shows the diurnal course of occurrence of different classes of auroras. The results obtained are consistent with the corresponding physical mechanisms and earlier studies [Nanjo et al., 2022; Vorobev et al., 2023].

Fig. 5.

For example, statistics indicate that auroras on the horizon (Fig. *5a*) are most likely to occur in the pre- and post-midnight hours, while observing an arc (Fig. *5b*) or discrete auroras (Fig. *5c*) is justified at midnight. The situation seems to be explained by the movement (relative to the observer) of the auroral oval from east to west (pre-midnight and post-midnight maxima, respectively). The auroras on the horizon at midnight are observed predominantly in the north and south and are caused by the latitudinal drift of the auroral zone boundaries.

The observation of auroras during cloudiness (Fig. *2e*) reflects an integral (for all types of auroras) probability distribution pattern, which has the highest symmetry relative to the local midnight and has the maximum standard deviation along the time axis (Fig. *5d*). In contrast, discrete (to a lesser extent arc) auroras have a pronounced excess in the vicinity of midnight, with the distance from which the probability of their observation sharply decreases.

The heterogeneity of the statistics of diffuse auroras (Fig. *5d*) can again be explained by the difficulties associated with their identification and, as a consequence, by the sensitive fraction of inclusions, false positives and false negatives.

A preliminary comparison of the HIT level registered at the 330 kV Vykhodnaya substation (68.83° N, 33.08° E) of the Northern Transit main power grid (http://gic.en51.ru) [Selivanov et al., 2023] with the classification results revealed that during the periods of discrete auroras the HIT level with a probability of 7.5% exceeds the threshold of 10 A, while during diffusion-type auroras the probability of reaching 10 A is only 0.31%.

Also the statistics considered in the first approximation indicates that during the periods of discrete auroras the HIT level with a probability of 50% exceeds 2.58 A. With the same probability during the auroras of the "arc" type, the HITs overcome the threshold of 0.98 A. During periods of diffuse auroras or in the absence of auroras as such, the HIT level with a probability of 50% does not exceed 0.72 and 0.41 A, respectively.

7. DISCUSSION OF RESULTS

The proposed classification approach, realized in ensemble with accumulated statistics of space weather effects on high-latitude technological systems, can be used in the tasks of hardware-free assessment of technosphere risks, failures and failures.

Unpretentiousness, autonomy, relatively low cost and ease of operation of all-sky cameras provide a global trend of growth in the number of information sources of this kind. Obviously, along with this, there is an increasing need for efficient solutions that automatically analyze and classify the recorded information, detect hidden patterns, and formulate preliminary conclusions.

The quality metrics achieved in this work demonstrate a high relevance of the results generated at the output of the information system, but additional research is required to investigate the issues related to the applicability of this approach to images obtained using different hardware from the hardware used at the LOZ station.

7. CONCLUSION

For most high-latitude regions of Russia (due to the lack of sufficient coverage by reliable sources of operational information on the local geomagnetic situation), auroras remain practically the only publicly available indicator of space weather conditions.

There are studies indicating that the area of polar lights observation, their luminescence intensity and morphology correlate with the power of manifestation of space weather effects on high-latitude technological systems.

Based on the ResNet50 deep convolutional neural network architecture and pre-trained on the Imagenet dataset, the information system provides ~96% accuracy in aurora classification, which is practically unattainable with manual or semi-automatic processing of large amounts of data.

The statistics considered in the first approximation indicates that during the periods of observation of discrete auroras with a probability of 7.5% the GIT level exceeds 10 A, while during diffusion auroras the probability of reaching the same level is 24 times lower.

Thus, the proposed approach to automatic classification of polar auroras can be applied in the tasks of hardware-free diagnostics of the upper ionosphere, technospheric risk assessment, and as a decision support tool for conducting relevant studies.

The result of automatic image classification based on the proposed system is available at: (https://disk.yandex.ru/i/76OMyWR4YyVYuw).

ACKNOWLEDGEMENTS

The authors are grateful to the Polar Geophysical Institute (PGI) for providing data on the observation of polar auroras obs. Lovozero, as well as the reviewers for constructive comments that allowed to improve the work significantly.

FUNDING

The work was supported by the Russian Science Foundation (project No. 21-77-30010-P).

REFERENCES

1. *Vorobyov A.V., Lapin A.N., Vorobyova G.R.* Software for automated recognition and digitization of archived optical aurora observations // Informatics and Automation. V. 22. No. 5. P. 1177-1206. 2023. https://doi.org/10.15622/ia .22.5.8

2. *Selivanov V.N., Aksenovich T.V., Bilin V.A., Kolobov V.V., Sakharov Ya.A.* Database of geo-induced currents in the main electric network "Northern Transit" // Solar-terrestrial physics. V. 9. No. 3. P. 100-110. 2023. https://doi.org/10.12737/szf-93202311

3. *Clausen L.B.N., Nickisch H.* Automatic classification of auroral images from the Oslo Auroral THEMIS (OATH) data set using machine learning // J. Geophys. Res − Space. V. 123. № 7. P. 5640−5647. 2018. https://doi.org/10.1029/2018JA025274

4. *Deng J., Dong W., Socher R., Li L.-J., Li K. Fei-Fei L.* ImageNet: A large-scale hierarchical image database / Proc. IEEE Conference on Computer Vision and Pattern Recognition (CVPR). June 20−25, 2009. Miami, FL. P. 248−255. 2009. https://doi.org/10.1109/CVPR.2009.5206848

5. *De Diego I.M., Redondo A.R., Fernández R.R., Navarro J., Moguerza J.M.* General performance score for classification problems // Appl. Intell. V. 52. № 10. P. 12049−12063. 2022. https://doi.org/10.1007/s10489-021-03041-7

6. *Endo T., Matsumoto M.* Aurora image classification with deep metric learning // Sensors. V. 22. № 17. ID 6666. 2022. https://doi.org/10.3390/s22176666

7. *Gallardo-Lacourt B., Nishimura Y., Donovan E., Gillies D.M., Perry G.W., Archer W.E., Nava O.A., Spanswick E.L.* A statistical analysis of STEVE // J. Geophys. Res. − Space. V. 123 № 11. P. 9893−9905. 2018. https://doi.org/10.1029/2018JA025368

8. *Glorot X., Bengio Y.* Understanding the difficulty of training deep feedforward neural networks / Proc. Thirteenth International Conference on Artificial Intelligence and Statistics. May 13–15, 2010. Sardinia, Italy. Proceedings of Machine Learning Research. V. 9. P. 249−256. 2010.

9. *He K., Zhang X., Ren S., Sun J.* Deep residual learning for image recognition / Proc. 2016 IEEE Conference on Computer Vision and Pattern Recognition (CVPR). June 26 – July 1, 2016. Las Vegas. V. P. 770−778. 2016. https://doi.org/10.1109/CVPR.2016.90

10. *Kvammen A., Wickstrøm K., McKay D., Partamies N.* Auroral image classification with deep neural networks // J. Geophys. Res. − Space. V. 125. № 10. ID e2020JA027808. 2020. https://doi.org/10.1029/2020JA027808

11. *Lian J., Liu T., Zhou Y.* Aurora classification in all-sky images via CNN–transformer // Universe. V. 9. № 5. ID 230. 2023. https://doi.org/10.3390/universe9050230

12. *MacDonald E. A., Donovan E., Nishimura Y. et al.* New science in plain sight: Citizen scientists lead to the discovery of optical structure in the upper atmosphere // Science Advances. V. 4. N 3. ID eaaq0030. 2018. https://doi.org/10.1126/sciadv.aaq0030

13. *Nanjo S., Nozawa S., Yamamoto M., Kawabata T., Johnsen M. G., Tsuda T.T., Hosokawa K.* An automated auroral detection system using deep learning: real-time operation in Tromsø, Norway // Scientific Reports. V. 12. ID 8038. 2022. https://doi.org/10.1038/s41598-022-11686-8

14. *Pilipenko V.A., Chernikov A.A., Soloviev A.A., Yagova N.V., Sakharov Y.A., Kudin D.V., Kostarev D.V., Kozyreva O.V., Vorobev A.V., Belov A.V.* Influence of space weather on the reliability of the transport system functioning at high latitudes // Russian Journal of Earth Sciences. V. 23. № 2. P. 1−34. 2023. https://doi.org/10.2205/2023ES000824

15. *Sado P., Clausen L.B.N., Miloch W.J., Nickisch H.* Transfer learning aurora image classification and magnetic disturbance evaluation // J. Geophys. Res. − Space. V. 127. № 1. ID e2021JA029683. 2022. https://doi.org/10.1029/2021JA029683

16. *Shorten C., Khoshgoftaar T.M.* A survey on image data augmentation for deep learning // Journal of Big Data. V. 6. ID 60. 2019. https://doi.org/10.1186/s40537-019-0197-0

17. *Steven R., Barnes M., Garnett S.T., Garrard G., O'Connor J., Oliver J.L., Robinson C., Tulloch A., Fuller R.A.* Aligning citizen science with best practice: Threatened species conservation in Australia // Conservation Science and Practice. V. 1. № 10. ID e100. 2019. https://doi.org/10.1111/csp2.100

18. *Vorobev A.V., Lapin A.N., Soloviev A.A., Vorobeva G.R.* An approach to interpreting space weather natural indicators to evaluate the impact of space weather on high-latitude power systems // Izv. Phys. Solid Eart. V. 60. № 4. P. 604−611. 2024. https://doi.org/10.1134/S106935132470054X

19. *Vorobev A.V., Soloviev A.A., Pilipenko V.A., Vorobeva G.R., Gainetdinova A.A., Lapin A.N., Belahovskiy V.B., Roldugin A.V.* Local diagnostics of aurora presence based on intelligent analysis of geomagnetic data // Solar-Terrestrial Physics. V. 9. № 2. P. 22−30. 2023. https://doi.org/10.12737/stp-92202303

20. *Vorobev A., Soloviev, A., Pilipenko V., Vorobeva G., Sakharov Y.* An approach to diagnostics of geomagnetically induced currents based on ground magnetometers data // Applied Sciences. V. 12. № 3. ID 1522. 2022. https://doi.org/10.3390/app12031522

21. *Yarotsky D.* Error bounds for approximations with deep ReLU networks // Neural Networks. V. 94. P. 103−114. 2017. https://doi.org/10.1016/j.neunet.2017.07.002

22. *Zhong Y., Huang R., Zhao J., Zhao B., Liu T.* Aurora image classification based on multi-feature latent Dirichlet allocation // Remote Sensing. V. 10. № 2. ID 233. 2018. https://doi.org/10.3390/rs10020233

Table 1. Classification systems for all-sky camera images

Arc	Diffuse	Discrete	Cloudy	Clear No aurora	Other classes	Source
+	-	-	-	+	Radiation corona, Hot-spot corona, Drapery corona	[Zhong et al., 2018].
+	+	+	+	+	Moon	[Clausen and Nickisch, 2018]
+	+ (Patchy)	+	-	+ (Faint)	Breakup, Colored, Edge,	[Kvammen et al., 2020].
+	+	+	+	+	Moon	[Endo and Matsumoto, 2022]
+	+	+	+	+	Aurora but Bright, Aurora but Cloudy, Dusk and Dawn.	[Nanjo et al., 2022]
+	+	+	+	+	Moon	[Sado et al., 2022]
+	+	+	+	+	Moon	[Lian et al., 2023]

Table 2. Ratio of occurrence of images belonging to different classes recorded by the obs camera. LOZ

Occurrence	Class						
	Clear sky	Discrete auroras	Arc	Diffuse aurora	Glow over the horizon	Glow and cloudy	Defective images
N	51 278	1 201	3 078	2 806	5 908	24 560	4 159
P, %	55.1	1.3	3.3	3.0	6.4	26.4	4.5

Note: N - number of events of the given class; *P* - share of the total number of events.

Table 3. Matrix of image classification inconsistencies

Truth	ANN						
	Glows and cloudy	Arc glow	Defective images	Diffuse	Discrete	Clear sky/ no auroras	Auroras over the horizon
Lights and cloudy	93.5	0.1	0.0	0.2	0.1	6.0	0.2
Arc glow	1.0	92.9	0.0	1.4	2.0	1.5	1.2
Defective images	0.2	0.0	99.8	0.0	0.0	0.0	0.0
Diffuse radiance	2.2	7.5	0.0	75.2	3.1	7.5	4.6
Discrete radiance	1.3	7.1	0.0	0.9	89.7	0.4	0.4
Clear skies/ no auroras	0.4	0.0	0.0	0.0	0.0	99.4	0.1
Lights over the horizon	1.4	2.6	0.0	0.7	0.0	3.1	92.2

Table 4. Quality metrics of the polar lights classification system

Class	Metric			
	Recall, %	Precision, %	F1, %	Number images
Glow and cloudy	93	98	96	4933
Arc radiance	93	85	89	589
Defective images	100	100	100	817
Diffuse glow	75	94	83	548
Discrete glow	90	86	88	224
Clear skies / no auroras	99	96	98	10292
Auroras over the horizon	92	95	94	1154
Total weighted	96	96	96	18557
Total macro-averaged	92	93	92	18557

FIGURE CAPTIONS

Fig. 1. State of the sky registered by the all-sky camera of obs. Lovozero during December 21, 2016: (*a*) no auroras; (*b*) diffusion auroras; (*c*) auroras of the "arc" type; (*d*) *auroras* of the "vortex" type.

Fig. 2. Characteristic representatives of the classes of images considered in this work: (*a*) clear sky; (*b*) arc; (*c*) discrete auroras; (*d*) diffusion auroras; (*e*) auroras over the horizon; (*f*) auroras and cloudy; *(g*) defective images (images taken from the PIG resource (http://aurora.pgia.ru:8071/?p=2)).

Fig. 3. Examples of combined auroras: (*a*) superposition of diffuse and arc aurora, identified according to the proposed rule as arc aurora; (*b*) arc aurora observed near the horizon, identified as aurora on the horizon.

Fig. 4. ResNet50 network architecture.

Fig. 5. Daily course of occurrence of auroras of different classes: (*a*) aurora on the horizon; (*b*) arc aurora; (*c*) discrete aurora; (*d*) aurora and cloud cover; (*e*) diffuse auroras.

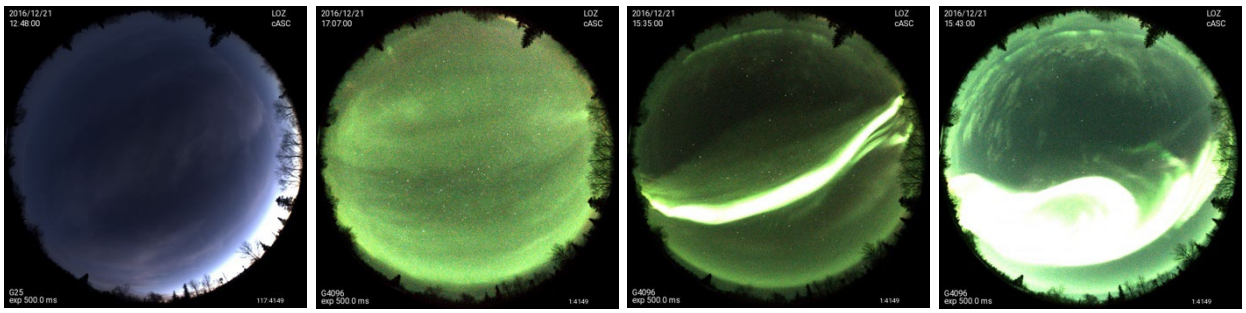

a *b* *c* *d*

Fig. 1.

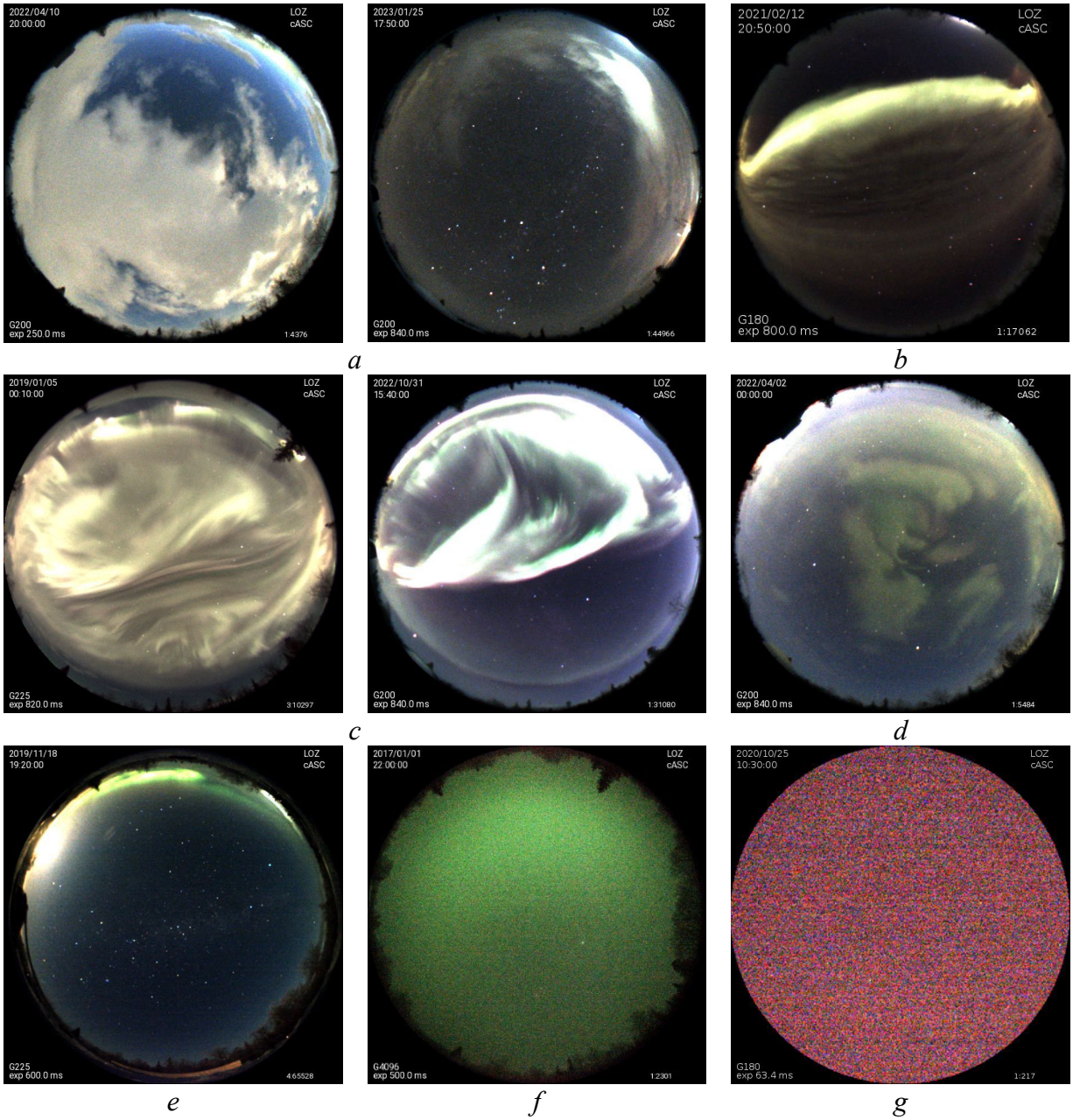

a *b* *c* *d* *e* *f* *g*

Fig. 2.

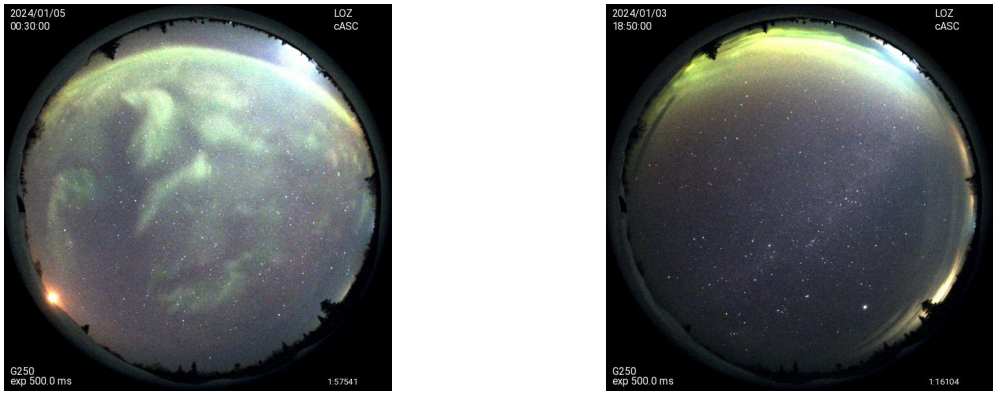
2024/01/05
00:30:00
LOZ
cASC
G250
exp 500.0 ms
1:57541
2024/01/03
18:50:00
LOZ
cASC
G250
exp 500.0 ms
1:16104

a *b*

Fig. 3.

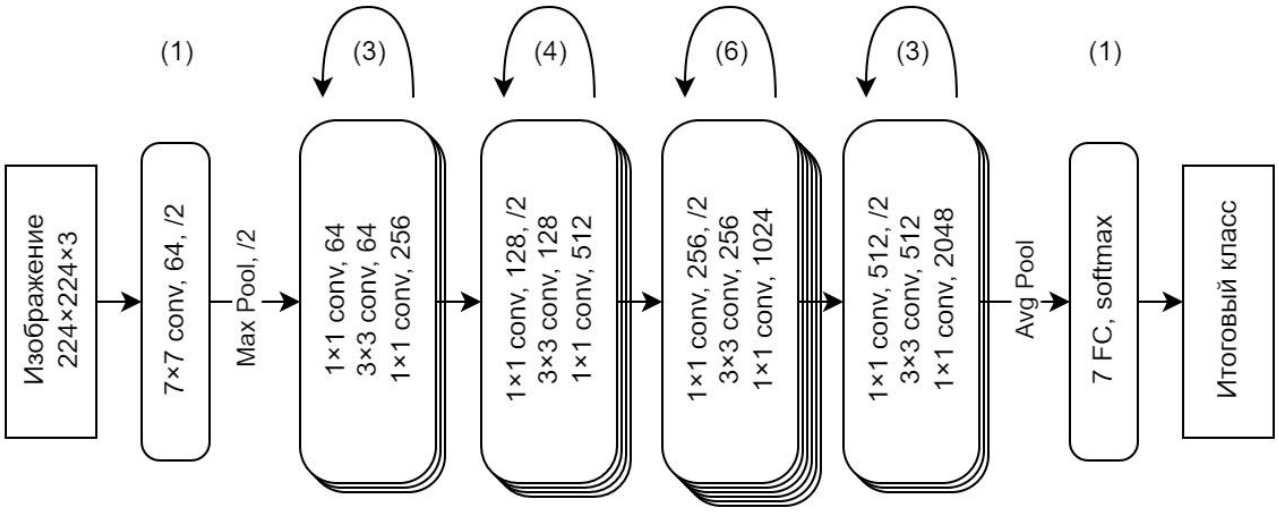
Изображение
224×224×3
(1)
7×7 conv, 64, /2
Max Pool, /2
(3)
1×1 conv, 64
3×3 conv, 64
1×1 conv, 256
(4)
1×1 conv, 128, /2
3×3 conv, 128
1×1 conv, 512
(6)
1×1 conv, 256, /2
3×3 conv, 256
1×1 conv, 1024
(3)
1×1 conv, 512, /2
3×3 conv, 512
1×1 conv, 2048
Avg Pool
(1)
7 FC, softmax
Итоговый класс

Fig. 4.

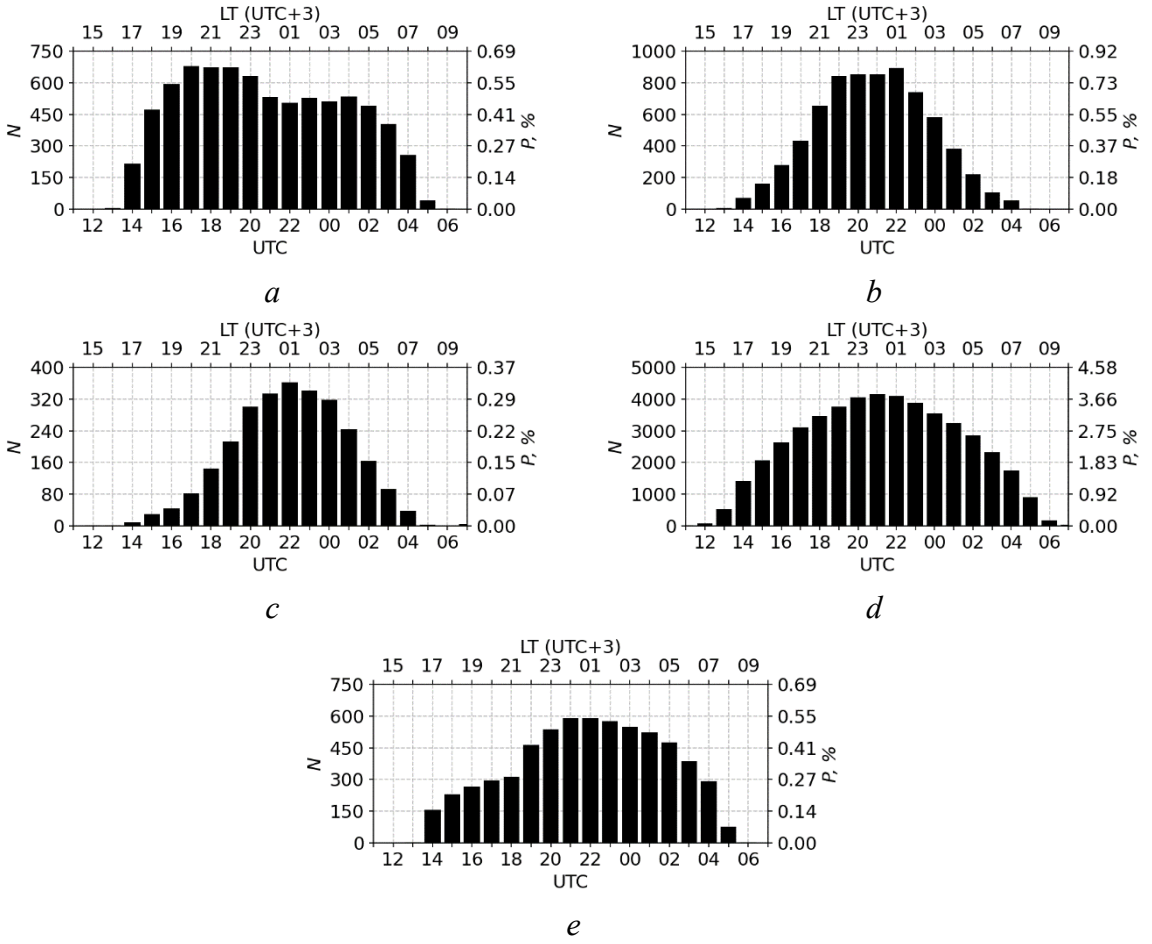
LT (UTC+3)
15 17 19 21 23 01 03 05 07 09
N
P, %
UTC
12 14 16 18 20 22 00 02 04 06
a
b
c
d
e

Fig. 5.